ACS OMEGA

http://pubs.acs.org/journal/acsodf

Article

Photooxidation Activity Control of Dimethylaminophenyl-tris-(*N*-methyl-4-pridinio)porphyrin by pH

Kazutaka Hirakawa,* Syunsuke Takai, Hiroaki Horiuchi, and Shigetoshi Okazaki

Cite This: *ACS Omega* 2020, 5, 27702−27708

Read Online

ACCESS | Metrics & More | Article Recommendations | Supporting Information

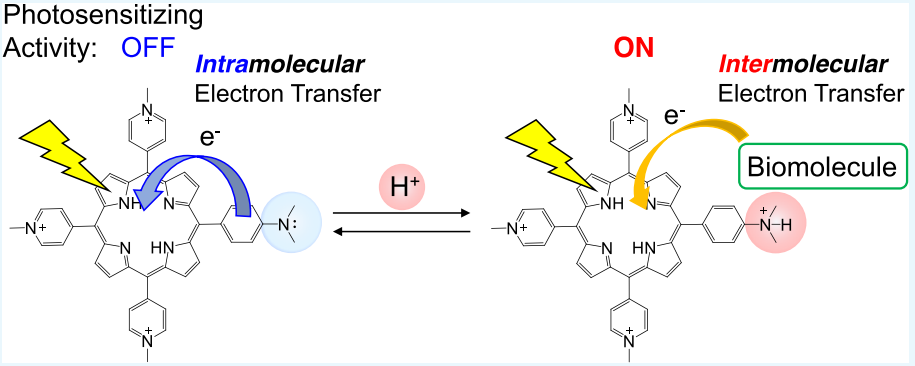

ABSTRACT: To control the activity of photodynamic agents by pH, an electron donor-connecting cationic porphyrin, *meso*-(*N*′,*N*′-dimethyl-4-aminophenyl)-tris(*N*-methyl-*p*-pyridinio)porphyrin (DMATMPyP), was designed and synthesized. The photoexcited state (singlet excited state) of DMATMPyP was deactivated through intramolecular electron transfer under a neutral condition. The pK_a of the protonated DMATMPyP was 4.5, and the fluorescence intensity and singlet oxygen-generating activity increased under an acidic condition. Furthermore, the protonation of DMATMPyP enhanced the biomolecule photooxidative activity through electron extraction. Photodamage of human serum albumin (HSA) was observed under a neutral condition because a hydrophobic HSA environment can reverse the deactivation of photoexcited DMATMPyP. However, an HSA-damaging mechanism of DMATMPyP under a neutral condition was explained by singlet oxygen production. Therefore, it is indicated that the protein photodamaging activity of DMATMPyP goes into an OFF state under a neutral hypoxic condition. Under an acidic condition, the HSA photodamaging quantum yield by DMATMPyP through electron extraction could be preserved in the presence of a singlet oxygen quencher. Photooxidation of nicotinamide adenine dinucleotide by DMATMPyP was also enhanced under an acidic condition. This study demonstrated the concept of using pH to control photosensitizer activity via inhibition of the intramolecular electron transfer deactivation and enhancement of the oxidative activity through the electron extraction mechanism. Specifically, biomolecule oxidation through electron extraction may play an important role in photodynamic therapy to treat tumors under a hypoxic condition.

INTRODUCTION

Electron transfer is the key factor in controlling the photochemical process of photoexcited molecules.[1−6] Fluorescence sensing,[7−9] bioimaging,[10−14] singlet oxygen ($^1O_2$) production,[15−21] and photooxidative activities[22] of photoexcited molecules can be controlled through intramolecular electron transfer. Changes in the redox potential of a molecule by its surroundings, for example, pH,[9,18−22] metal ion concentration,[7,8] and interaction with macromolecules, such as DNA,[15−17] can inhibit the electron-transfer quenching, leading to an active (ON) state. One important application of the OFF → ON control is in the photomedicinal property of molecules. For example, cancer-selective photodynamic therapy (PDT) can be realized by controlling the activity of photosensitizing molecules (photosensitizers). PDT is a less-invasive treatment for cancer and other nonmalignant conditions.[5,23−27] Administered photosensitizers are illuminated by nonthermal visible light, resulting in biomolecule damage through photochemical reactions. In general, $^1O_2$ production through energy transfer from the excited photosensitizer to oxygen molecules is considered to be an important mechanism in biomolecule damage.[28,29] Electron transfer from biomolecules to the photoexcited photosensitizers can be an alternate mechanism of PDT.[30−32] It has been reported that

Received: September 3, 2020
Accepted: September 29, 2020
Published: October 12, 2020

https://dx.doi.org/10.1021/acsomega.0c04303
ACS Omega 2020, 5, 27702−27708

the pH of cancer cells is slightly acidic because of the enhancement of glycolysis.[33−35] As mentioned above, electron transfer can be controlled by pH. Furthermore, in general, a protonated cationic compound becomes a stronger electron acceptor than its nonprotonated form.[36] Therefore, the pH-induced change in the intramolecular electron transfer can be applied to cancer-selective PDT.[18−22] The aim of this study is to examine the concept of using pH to control the activity of a cationic water-soluble porphyrin photosensitizer. Tetrakis(*N*-methyl-*p*-pyridinio)porphyrin (TMPyP) has been studied as the model compound for PDT.[17,29] Because the water-solubility of previously reported porphyrins was relatively low,[18−20,22] the use of TMPyP-based porphyrin may be advantageous for the application. To control the photosensitizing activity of TMPyP, *meso*-(*N*′,*N*′-dimethyl-4-aminophenyl)-tris(*N*-methyl-*p*-pyridinio)porphyrin (DMATMPyP, Figure 1)

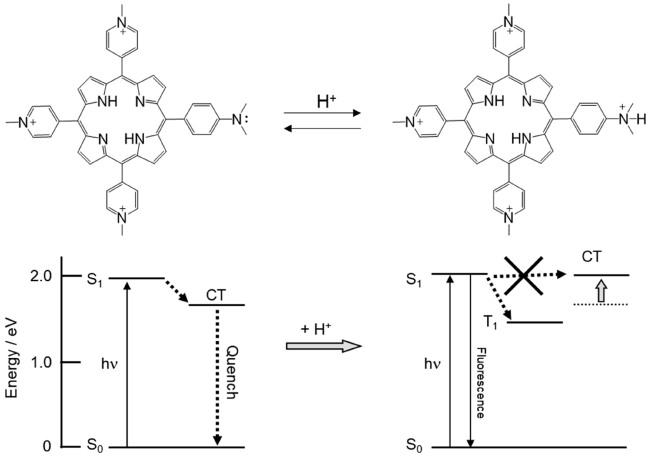

Figure 1. Molecular structure and the proposed relaxation schemes of DMATMPyP and the protonated form (H^+-DMATMPyP).

was designed and synthesized. The dimethylaniline (DMA) moiety was used as a pH-dependent electron donor. The photochemical property and biomolecule-damaging activity of DMATMPyP were examined.

RESULTS

Energy Level of the Intramolecular Charge Transfer State. The structures of DMATMPyP and its protonated form (H^+-DMATMPyP) were optimized using density functional theory (DFT) calculation at the ωB97X-D/6-31G* level (Supporting Information). Their orbital energies were also calculated. These calculations showed that the highest occupied molecular orbital (HOMO) of DMATMPyP is located on the DMA moiety (Supporting Information). Consequently, it is speculated that the photoexcited state of DMATMPyP can be deactivated via intramolecular electron transfer from the DMA moiety to the porphyrin ring, forming a charge-transfer (CT) state (Figure 1). In the case of H^+-DMATMPyP, the HOMO is located on the porphyrin ring, suggesting that the electron transfer-mediated quenching can be suppressed under an acidic condition. In addition, the highest molecular orbital energy of the porphyrin ring of H^+-DMATMPyP (−17.4 eV, in vacuum, calculated using the DFT method) became lower than that of DMATMPyP (−12.9 eV).

Gibbs Energy of the Intramolecular Electron Transfer. The Gibbs energy (ΔG_{iet}) of the intramolecular electron transfer from the DMA moiety to the porphyrin ring was roughly calculated using the redox potentials and excitation energy of DMATMPyP (Supporting Information). The obtained value (ΔG_{iet} = −0.73 eV) supports the possibility of quenching through intramolecular electron transfer.

pK_a of the Protonated DMATMPyP. The UV−Vis absorption spectra of DMATMPyP shifted depending on pH (Figure 2A). This absorption spectral change of DMATMPyP by pH could be explained by the protonation of the DMA moiety and the central pyrrole nitrogen atoms.[37] Analysis of the relationship between absorbance and pH (Figure 3) was

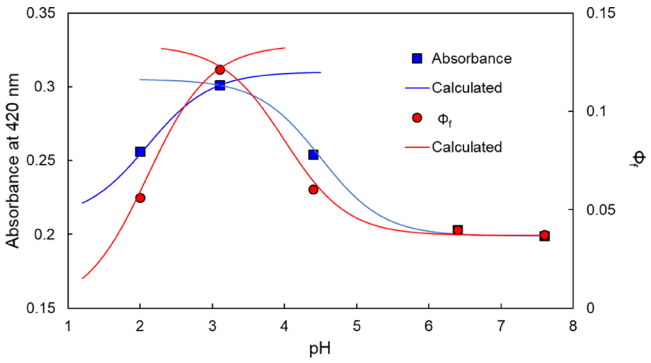

Figure 3. Relationship between the photochemical parameters of DMATMPyP (absorbance at 440 nm and fluorescence quantum yield) and the pH of the solvent. The sample solution contained 5 μM DMATMPyP in a 10 mM sodium phosphate buffer (indicated pH). The excitation wavelength was 550 nm. The method of analysis is described in the Supporting Information.

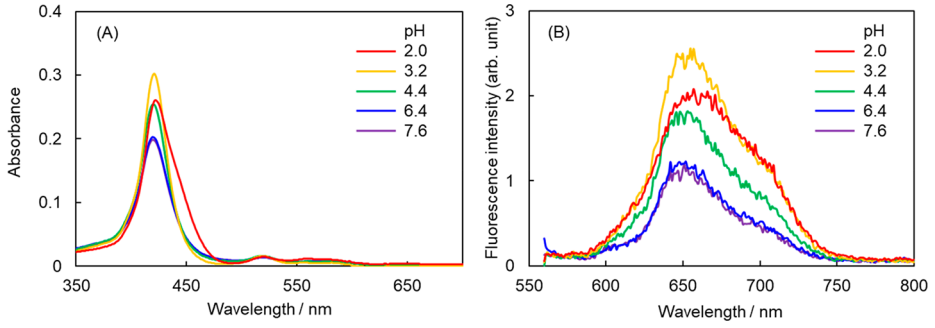

Figure 2. (A) Absorption and (B) fluorescence spectra of DMATMPyP. The sample solution contained 5 μM DMATMPyP in a 10 mM sodium phosphate buffer (indicated pH). The excitation wavelength was 550 nm.

https://dx.doi.org/10.1021/acsomega.0c04303
ACS Omega 2020, 5, 27702−27708

Table 1. Quantum Yields of Biomolecule Damage and $^1O_2$ Production Photosensitized by DMATMPyP[a]

pH	$\Phi_{HSA(T)}$	$\Phi_{HSA(ET)}$	$\Phi_{HSA(\Delta)}$	$\Phi_{NADH(T)}$	$\Phi_{NADH\ (ET)}$	$\Phi_{NADH(\Delta)}$	Φ_{Δ}
7.6	4.4×10^{-4}	~0	4.4×10^{-4}	0.03	0.023	0.007	0.18
3.2	1.6×10^{-4}	1.4×10^{-4}	0.2×10^{-4}	0.18	0.14	0.044	0.36

[a]$\Phi_{HSA(T)}$: total quantum yields of HSA damage; $\Phi_{HSA(ET)}$: quantum yield of HSA damage through electron transfer; $\Phi_{HSA(\Delta)}$: quantum yield of HSA damage through $^1O_2$ production; $\Phi_{NADH(T)}$: total quantum yields of NADH decomposition; $\Phi_{NADH\ (ET)}$: quantum yield of NADH decomposition through electron transfer; $\Phi_{NADH(\Delta)}$: quantum yield of NADH decomposition through $^1O_2$ production.

performed using a method similar to that in previous reports (Supporting Information).[22] The obtained pK_a values were 4.5 and 2.1. These values could be explained by the fact that the pK_a of H^+-DMATMPyP is 4.5 and that of the central nitrogen atoms is 2.1. Indeed, a similar pK_a value of the central nitrogen atoms has been reported in the case of a similar porphyrin.[37]

pH-Dependent Fluorescence Change. The fluorescence intensity was also changed by pH, and a relationship similar to that with the absorbance change was observed (Figure 3). A relatively small fluorescence quantum yield (Φ_f) value (0.037 at pH 7.6 and pH 6.4) under neutral conditions suggests the quenching of the singlet excited (S_1) state of the porphyrin ring through intramolecular electron transfer. The observed Φ_f value at pH 3.2 (0.12) was significantly larger than that under the neutral condition and suggests the inhibition of electron transfer-mediated quenching.

Triplet Excited-State Formation and $^1O_2$ Production. Transient absorption measurements showed the typical peak at around 470 nm,[38] which was assigned to the absorption spectrum of the triplet excited (T_1) state (Supporting Information). Enhancement of the T_1-state formation under an acidic condition was qualitatively demonstrated. $^1O_2$ production photosensitized by DMATMPyP was confirmed by near-infrared emission measurement, as previously reported (Supporting Information).[39] The calculated values of $^1O_2$ production quantum yield (Φ_Δ) are listed in Table 1. The analyzed time constant of $^1O_2$ emission showed that the lifetimes of $^1O_2$ were 3.8 μs (pH 7.6) and 3.9 μs (pH 3.2). These values were similar to the reported values for the $^1O_2$ lifetime in an aqueous solution.[17] Furthermore, these results showed that the lifetime of $^1O_2$ in an aqueous solution is barely affected by pH in this experimental region (pH 7.6−3.2). Indeed, the previous reports demonstrated that $^1O_2$ lifetime in deuterium oxide (72−78 μs)[40] is independent of acid concentration (72−77 μs in the presence of 5 mM trifluoroacetic acid).[36] The T_1 lifetime was also estimated from these emissions using the equation in the literature[41] (Supporting Information). The obtained values of T_1-state lifetimes were 1.6 μs (pH 7.6) and 1.3 μs (pH 3.2). These values were almost the same as the decay time of the T_1 transient absorption (about 1 μs, Supporting Information). The T_1-state lifetime is mostly determined by the quenching by oxygen molecules and becomes about 1−2 μs in an aqueous solution.[17,30]

Interaction between Human Serum Albumin and DMATMPyP. To investigate the protein photodamage by DMATMPyP using human serum albumin (HSA), their interaction was studied. The absorption spectra of DMATMPyP in the visible region were changed by the addition of HSA (Supporting Information). Since HSA has no absorption in the visible region, the absorption change can be explained by the binding interaction.[30−32] Analysis of the absorbance change by the previously reported method[30−32] showed that the binding constant (K_{bc}) under a neutral condition (3.3×10^6 M^{-1}, pH 7.6) was larger than that under an acidic condition (2.1×10^5 M^{-1}, pH 3.2). The distance between the binding DMATMPyP molecule and the tryptophan residue of HSA, which is located almost at the center of HSA, was estimated based on an analysis using the Förster resonance energy transfer (FRET) method based on the energy transfer theory[42] (Supporting Information). The obtained values were 57 and 55 Å under pH 7.6 and 3.2, respectively.

Photosensitized Protein Oxidation by DMATMPyP. The photosensitized protein oxidation activity of DMATMPyP was examined by a fluorescence intensity of HSA, as previously reported.[30−32] The abovementioned K_{bc} values showed that the binding ratios of DMATMPyP to HSA were 95% (pH 7.6) and 60% (pH 3.2) in this experimental condition (10 μM HSA and 5 μM DMATMPyP). The tryptophan residue of HSA can be an important indicator of protein oxidation. HSA has one tryptophan,[43] which is easily oxidized through electron transfer and $^1O_2$ generation, leading to the diminishment of its intrinsic fluorescence.[30−32] We observed that HSA photooxidation was irradiation-dose dependent (Figure 4). The extent of photosensitized HSA oxidation caused by DMATMPyP increased under a neutral condition. The quantum yields of HSA photodamage through $^1O_2$ generation and the electron transfer-mediated mechanism were examined in light of the scavenger effect of NaN_3, a strong physical quencher of $^1O_2$,[44] as in previous reports.[30−32] The photosensitized HSA damage increased linearly within 30 min. Therefore, the amount of HSA damage by DMATMPyP with NaN_3 for 30 min of photoirradiation was compared with that without NaN_3. The estimated quantum yields are listed in Table 1.

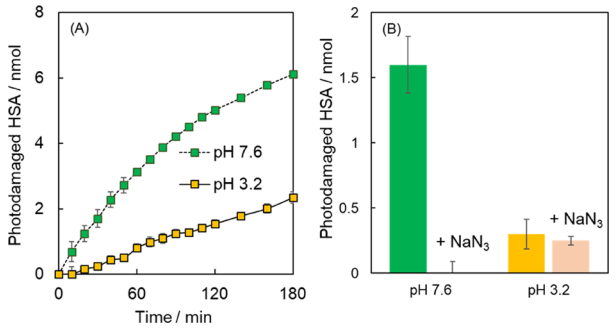

Figure 4. (A) Time profile of HSA damage photosensitized by DMATMPyP and (B) the effect of a $^1O_2$ quencher. The sample solution containing 10 μM HSA and 5 μM DMATMPyP with or without 10 mM NaN_3 in a 10 mM sodium phosphate buffer (indicated pH) was irradiated with an LED (585 nm, 2.0 mW cm^{-2}). The effect of NaN_3 was examined for 30 min photoirradiation. Data are presented as mean ± standard error (SE) (n = 3).

Photosensitized NADH Oxidation by DMATMPyP. Nicotinamide adenine dinucleotide (NADH) was used as the target biomolecule to examine the photosensitizing activity of DMATMPyP. NADH can be oxidized by $^1O_2$ production and electron transfer reactions.[22] Because NADH is a relatively

https://dx.doi.org/10.1021/acsomega.0c04303
ACS Omega 2020, 5, 27702−27708

small molecule and the binding interaction with DMATMPyP is considered to be negligibly small, an environmental effect such as the case of HSA does not occur. Therefore, relatively high concentration of NADH (100 μM) against DMATMPyP (5 μM) was used. The typical absorption spectrum of NADH, around 340 nm, was decreased by photoirradiation with DMATMPyP. The NADH photooxidation was increased under an acidic condition (Figure 5). Similar to the analysis

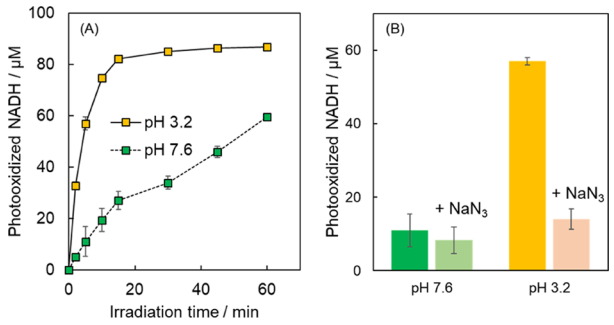

Figure 5. (A) Time profile of NADH oxidation photosensitized by DMATMPyP and (B) the effect of a $^1O_2$ quencher. The sample solution containing 100 μM NADH and 5 μM DMATMPyP with or without 10 mM NaN_3 in a 10 mM sodium phosphate buffer (indicated pH) was irradiated with an LED (585 nm, 2.0 mW cm^{-2}). The effect of NaN_3 was examined for 5 min photoirradiation. Data are presented as mean ± SE (n = 3).

of HSA damage, the NADH photooxidation by DMATMPyP with NaN_3 for 5 min of photoirradiation was compared with that without NaN_3. The estimated quantum yields of NADH oxidation photosensitized by DMATMPyP are listed in Table 1.

DISCUSSION

The photoexcited state (S_1 state) of DMATMPyP was deactivated through intramolecular electron transfer from the DMA moiety, the electron-donating moiety, in an aqueous solution. DFT calculation and the observed redox potentials supported this intramolecular electron transfer. The pK_a of the protonated DMA moiety of H^+-DMATMPyP was 4.5, and the fluorescence intensity was recovered in an acidic solution. DFT calculation predicted that the intramolecular electron transfer in H^+-DMATMPyP is suppressed because the highest occupied orbital energy of the DMA moiety becomes lower than that of the porphyrin ring. These results indicated that the relaxation process of the DMATMPyP S_1 state could be controlled by pH through protonation of the electron-donating moiety, as proposed in Figure 1. The photosensitized $^1O_2$-generating activity of DMATMPyP was increased under an acidic condition. Transient absorption spectrum measurements verified that T_1-state formation is enhanced under an acidic condition (Supporting Information). Inhibition of the S_1-state quenching leads to the increase in intersystem crossing efficiency to the T_1 state and $^1O_2$ generation.

The absorption spectral change showed that DMATMPyP bound to HSA. The tryptophan residue is located near the center of HSA,[43] and HSA has pockets as drug-binding sites (Sudlow's site I and site II).[45] The FRET method suggests that the distance between DMATMPyP and the tryptophan residue is almost 55 Å. Since the size of HSA is almost 100 Å,[43] this result suggests that DMATMPyP binds mostly to the surface of HSA pockets. The estimated binding constants between DMATMPyP and HSA under neutral (pH 7.6) and acidic (pH 3.2) conditions are 3.3×10^6 M^{-1} and 2.1×10^5 M^{-1}, respectively. HSA that is positively charged by the amino acid protonation under an acidic condition should inhibit the interaction with H^+-DMATMPyP.

Photoirradiation of DMATMPyP induced tryptophan residue damage. The estimated quantum yield of HSA damage at pH 7.6 was larger than that at pH 3.2. As mentioned above, a suppression of the interaction under an acidic condition may decrease the HSA damage by H^+-DMATMPyP at pH 3.2. Furthermore, a hydrophobic environment of protein is not appropriate for the intramolecular electron transfer because the CT-state energy level depends on the surrounding dielectric constant and increases in a less-polar environment.[46] The environment of HSA may lead to recovery of the photosensitizing activity of porphyrin. Therefore, the total HSA damage was decreased under an acidic condition. However,

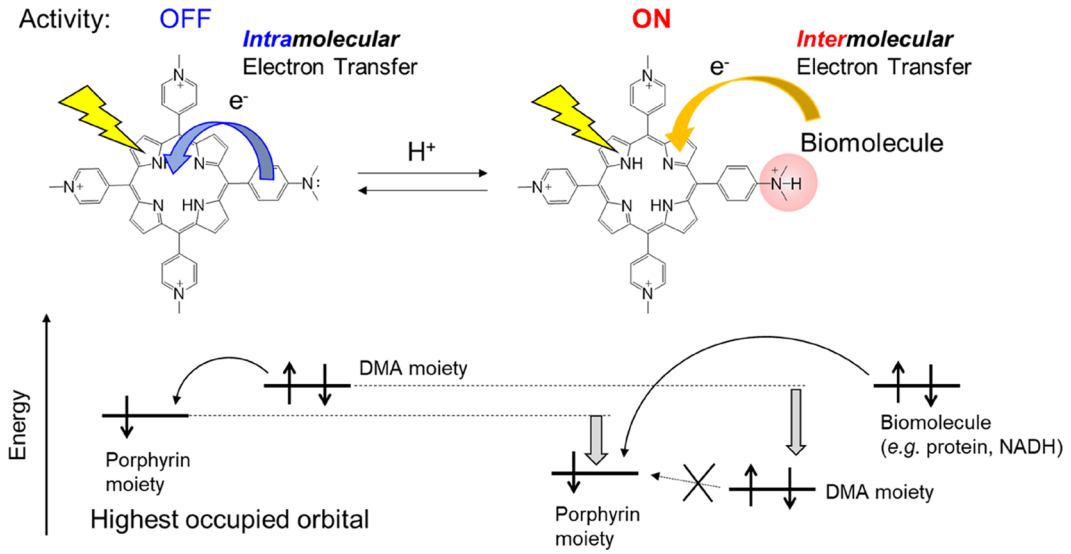

Figure 6. Diagram of the pH-controlled activity of the DMATMPyP photosensitizer and the relative energy levels of the highest occupied orbitals for the porphyrin moiety, DMA moiety, and targeting biomolecule.

https://dx.doi.org/10.1021/acsomega.0c04303
ACS Omega 2020, 5, 27702−27708

electron transfer-mediated HSA damage could be enhanced under an acidic condition. Analysis of the HSA-damaging quantum yield showed that the mechanism of HSA damage photosensitized by DMATMPyP at pH 7.6 is mainly explained by $^1O_2$ generation. The protein damage through $^1O_2$ production is suppressed under hypoxia in both cases of acidic and neutral conditions. However, the oxidative activity of DMATMPyP through the electron-transfer mechanism was enhanced under an acidic condition. DFT calculation showed that the molecular orbital energy level of the porphyrin ring becomes lower in the protonated state, H^+-DMATMPyP (Supporting Information). Consequently, photosensitized HSA damage by DMATMPyP through electron transfer could be preserved at pH 3.2 in the presence of a $^1O_2$ quencher. It is speculated that DMATMPyP can selectively oxidize proteins under an acidic hypoxic condition (Figure 6). NADH photooxidation was also induced by DMATMPyP. NADH is a relatively small biomolecule and does not form a binding complex with DMATMPyP. The results of NADH oxidation showed that the photooxidative activity of DMATMPyP can be increased under an acidic condition in a simple aqueous solution. Because NADH is easily oxidized, the observed quantum yield through the electron-transfer mechanism was not significantly increased under an acidic condition.

In summary, the relaxation process of DMATMPyP can be controlled by pH through the protonation of the DMA moiety. Fluorescence intensity, T_1-state formation, and the resulting Φ_Δ are increased in the H^+-DMATMPyP state. The total quantum yield of HSA photodamage was decreased under an acidic condition because the interaction between protonated HSA and H^+-DMATMPyP is weaker than that under a neutral condition and a hydrophobic environment reverses the photodamaging activity of DMATMPyP. However, under a hypoxic condition, DMATMPyP can selectively photosensitize protein damage through the electron transfer-mediated mechanism under an acidic condition since $^1O_2$-mediated biomolecule damage is not effective, whereas the electron transfer-mediated mechanism is enhanced by the protonation. Although the pK_a 4.5 of H^+-DMATMPyP is smaller than the physiological pH (around 7)[35] and not an ideal value for clinical use, this study demonstrated the concept of activity control based on inhibition of the intramolecular electron-transfer deactivation and enhancement of the oxidative activity through protonation of the photosensitizer. Specifically, electron transfer-mediated biomolecule oxidation can become an important PDT mechanism to treat tumors under a hypoxic condition.

EXPERIMENTAL SECTION

Materials. DMATMPyP was obtained by the methylation of *meso*-(*N*,*N*-dimethyl-4-aminophenyl)-tris(*p*-pyridyl)-porphyrin (DMATPyP). Synthesis of DMATPyP was according to the previously reported method.[47] To obtain DMATMPyP, the methylation of DMATPyP was carried out according to the literature.[48,49] Details about the synthesis and characterization of DMATMPyP are described in the Supporting Information. The spectroscopic-grade distilled water was purchased from Dojin Chemicals Co. (Kumamoto, Japan). Sodium phosphate buffer (pH 7.6) and NADH were from Nakalai Tesque Inc. (Kyoto, Japan). Dimethyl sulfoxide-d_6 and sodium azide were from FUJIFILM Wako Pure Chemical Co. (Osaka, Japan). Methyl iodide and diethyl ether were from Kanto Chemical Co., Inc. (Tokyo, Japan). HSA was purchased from Sigma-Aldrich Co. LLC. (St. Louis, MO, USA). These reagents were used as received. A sodium phosphate buffer (pH 6.4) was prepared from disodium hydrogen phosphate dodecahydrate and sodium dihydrogen phosphate dihydrate (Nacalai Tesque, Inc., Kyoto, Japan). Sodium phosphate buffers (pH 4.4 and 3.2) were prepared from sodium dihydrogen phosphate dihydrate (Nacalai Tesque, Inc.) and 0.05 M phosphoric acid (Kanto Chemical, Co. Inc., Tokyo. Japan). An acidic solution (pH 2.0) was prepared from 0.1 M hydrochloric acid solution (FUJIFILM Wako Pure Chemical Co.) and distilled water (FUJIFILM Wako Pure Chemical Co.).

Measurements. The absorption spectra of DMATMPyP were measured with a UV−Vis spectrophotometer UV-1650PC (Shimadzu, Kyoto, Japan). The fluorescence spectra of samples were measured with an F-4500 fluorescence spectrophotometer (Hitachi, Tokyo, Japan). The Φ_f was measured with an absolute photo-luminescence quantum yield measurement system (C9920-02, Hamamatsu Photonics KK, Hamamatsu, Japan). The $^1O_2$ formation photosensitized by DMATMPyP was directly measured by near-infrared luminescence around at 1270 nm from deactivated $^1O_2$, which corresponds to the $^1O_2$ ($^1\Delta_g$)-$^3O_2$($^3\Sigma_g^-$) transition as previously reported.[39] The Φ_Δ was determined from the comparison of the $^1O_2$ emission intensities by DMATMPyP solution and methylene blue (Φ_Δ = 0.52 in water).[50] A cyclic voltammogram was measured with a potentiostat/galvanostat (HA-301, Hokuto Denko Co., Tokyo, Japan), a function generator (DF1906, NF Co., Yokohama, Japan), and a data logger (midi LOGGER, GL900-4, Graphtec Co., Yokohama, Japan) using a platinum working electrode (ALS Co., Ltd., Tokyo, Japan), a platinum counterelectrode (ALS Co., Ltd), and saturated calomel electrode (SCE, ALS Co., Ltd).

Calculations. The optimized structure and energy of DMATMPyP and H^+-DMATMPyP were calculated by the DFT method at the ωB97X-D/6-31G* level utilizing the Spartan 18′ (Wavefunction Inc., CA, USA).

ASSOCIATED CONTENT

Supporting Information

The Supporting Information is available free of charge at https://pubs.acs.org/doi/10.1021/acsomega.0c04303.

Synthesis of DMATPyP and DMATMPyP, DFT calculation, calculation of the driving force of electron transfer, analysis of the pK_a values of DMATMPyP, transient absorption spectra of DMATMPyP, photosensitized singlet oxygen production by DMATMPyP, analysis of the interaction between DMATMPyP and HSA, and analysis of the binding position by the FRET method (PDF)

AUTHOR INFORMATION

Corresponding Author

Kazutaka Hirakawa − *Applied Chemistry and Biochemical Engineering Course, Department of Engineering, Graduate School of Integrated Science and Technology and Department of Optoelectronics and Nanostructure Science, Graduate School of Science and Technology, Shizuoka University, Hamamatsu 432-8561, Japan*; orcid.org/0000-0002-3694-8165; Phone: +81-53-478-1287; Email: hirakawa.kazutaka@shizuoka.ac.jp; Fax: +81-53-478-1287

https://dx.doi.org/10.1021/acsomega.0c04303
ACS Omega 2020, 5, 27702−27708

Authors

Syunsuke Takai − *Applied Chemistry and Biochemical Engineering Course, Department of Engineering, Graduate School of Integrated Science and Technology, Shizuoka University, Hamamatsu 432-8561, Japan*

Hiroaki Horiuchi − *Division of Molecular Science, Graduate School of Science and Technology, Gunma University, Kiryu 376-8515, Japan*

Shigetoshi Okazaki − *Preeminent Medical Photonics Education & Research Center, Hamamatsu University School of Medicine, Hamamatsu 431-3192, Japan*

Complete contact information is available at: https://pubs.acs.org/10.1021/acsomega.0c04303

Notes

The authors declare no competing financial interest.

■ ACKNOWLEDGMENTS

The authors wish to thank Dr. Hirohiko Watanabe and Dr. Kiyotada Hosokawa (Hamamatsu Photonics K.K.) for transient absorption measurement. The presented work was partially supported by Grants-in-Aid for Scientific Research (B) from Japan Society for the Promotion of Science (JSPS KAKENHI 17H03086) and Futaba Electronics Memorial Foundation (10407).

■ REFERENCES

(1) Wasielewski, M. R. Photoinduced Electron Transfer in Supramolecular Systems for Artificial Photosynthesis. *Chem. Rev.* **1992**, *92*, 435−461.

(2) Zhang, R.; Wu, Y.; Wang, Z.; Xue, W.; Fu, H.; Yao, J. Effects of Photoinduced Electron Transfer on the Rational Design of Molecular Fluorescence Switch. *J. Phys. Chem. C* **2009**, *113*, 2594−2602.

(3) Dadashi-Silab, S.; Doran, S.; Yagci, Y. Photoinduced Electron Transfer Reactions for Macromolecular Syntheses. *Chem. Rev.* **2016**, *116*, 10212−10275.

(4) Fujitsuka, M.; Majima, T. Reaction Dynamics of Excited Radical Ions Revealed by Femtosecond Laser Flash Photolysis. *J. Photochem. Photobiol., C* **2018**, *35*, 25−37.

(5) Roy, I.; Bobbala, S.; Young, R. M.; Beldjoudi, Y.; Nguyen, M. T.; Cetin, M. M.; Cooper, J. A.; Allen, S.; Anamimoghadam, O.; Scott, E. A.; Wasielewski, M. R.; Stoddart, J. F. A Supramolecular Approach for Modulated Photoprotection, Lysosomal Delivery, and Photodynamic Activity of a Photosensitizer. *J. Am. Chem. Soc.* **2019**, *141*, 12296−12304.

(6) Kim, J.; Oh, J.; Park, S.; Zafra, J. L.; DeFrancisco, J. R.; Casanova, D.; Lim, M.; Tovar, J. D.; Casado, J.; Kim, D. Two-electron Transfer Stabilized by Excited-state Aromatization. *Nat. Commun.* **2019**, *10*, 4983.

(7) de Silva, A. P.; Moody, T. S.; Wright, G. D. Fluorescent PET (Photoinduced Electron Transfer) Sensors as Potent Analytical Tools. *Analyst* **2009**, *134*, 2385−2393.

(8) Daly, B.; Ling, J.; de Silva, A. P. Current Developments in Fluorescent PET (photoinduced electron transfer) Sensors and Switches. *Chem. Soc. Rev.* **2015**, *44*, 4203−4211.

(9) Rosenberg, M.; Junker, A. K. R.; Sørensen, T. J.; Laursen, B. W. Fluorescence pH Probes Based on Photoinduced Electron Transfer Quenching of Long Fluorescence Lifetime Triangulenium Dyes. *ChemPhotoChem* **2019**, *3*, 233−242.

(10) Urano, Y.; Asanuma, D.; Hama, Y.; Koyama, Y.; Barrett, T.; Kamiya, M.; Nagano, T.; Watanabe, T.; Hasegawa, A.; Choyke, P. L.; Kobayashi, H. Selective Molecular Imaging of Vable Cancer Cells with pH-activatable Fluorescence Probes. *Nat. Med.* **2009**, *15*, 104−109.

(11) Sakabe, M.; Asanuma, D.; Kamiya, M.; Iwatate, R. J.; Hanaoka, K.; Terai, T.; Nagano, T.; Urano, Y. Rational Design of Highly Sensitive Fluorescence Probes for Protease and Glycosidase Based on Precisely Controlled Spirocyclization. *J. Am. Chem. Soc.* **2013**, *135*, 409−414.

(12) Piao, W.; Hanaoka, K.; Fujisawa, T.; Takeuchi, S.; Komatsu, T.; Ueno, T.; Terai, T.; Tahara, T.; Nagano, T.; Urano, Y. Development of an Azo-Based Photosensitizer Activated under Mild Hypoxia for Photodynamic Therapy. *J. Am. Chem. Soc.* **2017**, *139*, 13713−13719.

(13) Yoshihara, T.; Hirakawa, Y.; Hosaka, M.; Nangaku, M.; Tobita, S. Oxygen Imaging of Living Cells and Tissues Using Luminescent Molecular Probes. *J. Photochem. Photobiol., C* **2017**, *30*, 71−95.

(14) Zhu, H.; Hamachi, I. Fluorescence Imaging of Drug Target Proteins Using Chemical Probes. *J. Pharm. Anal.* in press, **2020**, DOI: DOI: 10.1016/j.jpha.2020.05.013.

(15) Cló, E.; Snyder, J. W.; Ogilby, P. R.; Gothelf, K. V. Control and Selectivity of Photosensitized Singlet Oxygen Production: Challenges in Complex Biological Systems. *ChemBioChem* **2007**, *8*, 475−481.

(16) Tørring, T.; Toftegaard, R.; Arnbjerg, J.; Ogilby, P. R.; Gothelf, K. V. Reversible pH-regulated Control of Photosensitized Singlet Oxygen Production Using a DNA i-Motif. *Angew. Chem. Int. Ed. Engl.* **2010**, *49*, 7923−7925.

(17) Hirakawa, K.; Nishimura, Y.; Arai, T.; Okazaki, S. Singlet Oxygen Generating Activity of an Electron Donor Connecting Porphyrin Photosensitizer Can Be Controlled by DNA. *J. Phys. Chem. B* **2013**, *117*, 13490−13496.

(18) Horiuchi, H.; Kuribara, R.; Hirabara, A.; Okutsu, T. pH-Response Optimization of Amino-Substituted Tetraphenylporphyrin Derivatives as pH-Activatable Photosensitizers. *J. Phys. Chem. A* **2016**, *120*, 5554−5561.

(19) Horiuchi, H.; Hirabara, A.; Okutsu, T. Importance of the Orthogonal Structure between Porphyrin and Aniline Moieties on the pH-Activatable Porphyrin Derivative for Photodynamic Therapy. *J. Photochem. Photobiol., A* **2018**, *365*, 60−66.

(20) Horiuchi, H.; Isogai, M.; Hirakawa, K.; Okutsu, T. Improvement of the ON/OFF Switching Performance of a pH-Activatable Porphyrin Derivative by the Introduction of Phosphorus(V). *ChemPhotoChem* **2019**, *3*, 138−144.

(21) Radunz, S.; Wedepohl, S.; Röhr, M.; Calderón, M.; Tschiche, H. R.; Resch-Genger, U. pH-Activatable Singlet Oxygen-Generating Boron-dipyrromethenes (BODIPYs) for Photodynamic Therapy and Bioimaging. *J. Med. Chem.* **2020**, *63*, 1699−1708.

(22) Hirakawa, K.; Onishi, Y.; Ouyang, D.; Horiuchi, H.; Okazaki, S. pH-Dependent Photodynamic Activity of Bis(6-methyl-3-pyridylmethoxy)P(V)tetrakis(*p*-methoxyphenyl)porphyrin. *Chem. Phys. Lett.* **2020**, *746*, 137315.

(23) Dolmans, D. E. J. G. J.; Fukumura, D.; Jain, R. K. Photodynamic Therapy for Cancer. *Nat. Rev. Cancer* **2003**, *3*, 380−387.

(24) Castano, A. P.; Mroz, P.; Hamblin, M. R. Photodynamic Therapy and Anti-tumour Immunity. *Nat. Rev. Cancer* **2006**, *6*, 535−545.

(25) Galstyan, A.; Maurya, Y. K.; Zhylitskaya, H.; Bae, Y. J.; Wu, Y.-L.; Wasielewski, M. R.; Lis, T.; Dobrindt, U.; Stępień, M. p-Extended Donor−Acceptor Porphyrins and Metalloporphyrins for Antimicrobial Photodynamic Inactivation. *Chem. − Eur. J.* **2020**, *26*, 8262−8266.

(26) Ghorbani, J.; Rahban, D.; Aghamiri, S.; Teymouri, A.; Bahador, A. Photosensitizers in Antibacterial Photodynamic Therapy: An Overview. *Laser Ther.* **2018**, *27*, 293−302.

(27) Cecatto, R. B.; de Magalhães, L. S.; Rodrigues, M. F. S. D.; Pavani, C.; Lino-dos-Santos-Franco, A.; Gomes, M. T.; Silva, D. F. T. Methylene Blue Mediated Antimicrobial Photodynamic Therapy in Clinical Human Studies: The State of the Art. *Photodiagn. Photodyn. Ther.* **2020**, *31*, 101828.

(28) DeRosa, M. C.; Crutchley, R. J. Photosensitized Singlet Oxygen And Its Applications. *Coord. Chem. Rev.* **2002**, *233-234*, 351−371.

(29) Lang, K.; Mosinger, J.; Wagnerová, D. M. Photophysical Properties of Porphyrinoid Sensitizers Non-covalently Bound to Host Molecules; Models for Photodynamic Therapy. *Coord. Chem. Rev.* **2004**, *248*, 321−350.

(30) Hirakawa, K.; Umemoto, H.; Kikuchi, R.; Yamaguchi, H.; Nishimura, Y.; Arai, T.; Okazaki, S.; Segawa, H. Determination of Singlet Oxygen and Electron Transfer Mediated Mechanisms of Photosensitized Protein Damage by Phosphorus(V)porphyrins. *Chem. Res. Toxicol.* **2015**, *28*, 262−267.
(31) Hirakawa, K.; Ouyang, D.; Ibuki, Y.; Hirohara, S.; Okazaki, S.; Kono, E.; Kanayama, N.; Nakazaki, J.; Segawa, H. Photosensitized Protein-damaging Activity, Cytotoxicity, and Antitumor Effects of P(V)porphyrins Using Long-Wavelength Visible-light through Electron Transfer. *Chem. Res. Toxicol.* **2018**, *31*, 371−379.
(32) Hirakawa, K.; Suzuki, A.; Ouyang, D.; Okazaki, S.; Ibuki, Y.; Nakazaki, J.; Segawa, H. Controlled Photodynamic Action of Axial Fluorinated DiethoxyP(V)tetrakis(*p*-methoxyphenyl)porphyrin through Self-Aggregation. *Chem. Res. Toxicol.* **2019**, *32*, 1638−1645.
(33) Casey, J. R.; Grinstein, S.; Orlowski, J. Sensors and Regulators of Intracellular pH. *Nat. Rev. Mol. Cell Biol.* **2010**, *11*, 50−61.
(34) Webb, B. A.; Chimenti, M.; Jacobson, M. P.; Barber, D. L. Dysregulated pH: a Aerfect Storm for Cancer Progression. *Nat. Rev. Cancer* **2011**, *11*, 671−677.
(35) Persi, E.; Duran-Frigola, M.; Damaghi, M.; Roush, W. R.; Aloy, P.; Cleveland, J. L.; Gillies, R. J.; Ruppin, E. Systems Analysis of Intracellular pH Vulnerabilities for Cancer Therapy. *Nat. Commun.* **2018**, *9*, 2997.
(36) Hirakawa, K.; Hirano, T.; Nishimura, Y.; Arai, T.; Nosaka, Y. Control of Singlet Oxygen Generation Photosensitized by *meso*-Anthrylporphyrin through Interaction with DNA. *Photochem. Photobiol.* **2011**, *87*, 833−839.
(37) Fujimura, T.; Aoyama, Y.-H.; Sasai, R. Unique Protonation Behavior of Cationic Free-base Porphyrins in the Interlayer Space of Transparent Solid Films Comprising Layered A-zirconium Phosphate. *Tetrahedron Lett.* **2019**, *60*, 150912.
(38) Hirakawa, K.; Hosokawa, Y.; Nishimura, Y.; Okazaki, S. Relaxation Process of S_2 Excited Zinc Porphyrin through Interaction with a Directly Connected Phenanthryl Group. *Chem. Phys. Lett.* **2019**, *732*, 136652.
(39) Hirakawa, K.; Taguchi, M.; Okazaki, S. Relaxation Process of Photoexcited *meso*-Naphthylporphyrins while Interacting with DNA and Singlet Oxygen Generation. *J. Phys. Chem. B* **2015**, *119*, 13071−13078.
(40) Hirakawa, K.; Hirano, T.; Nishimura, Y.; Arai, T.; Nosaka, Y. Dynamics of Singlet Oxygen Generation by DNA-Binding Photosensitizers. *J. Phys. Chem. B* **2012**, *116*, 3037−3044.
(41) Krasnovsky, A. A., Jr. Luminescence and Photochemical Studies of Singlet Oxygen Photonics. *J. Photochem. Photobiol., A* **2008**, *196*, 210−218.
(42) Förster, T. Zwischenmolekulare Energiewanderung und Fluoreszenz. *Ann. Phys.* **1948**, *437*, 55−75.
(43) He, X. M.; Carter, D. C. Atomic Structure and Chemistry of Human Serum Albumin. *Nature* **1992**, *358*, 209−215.
(44) Li, M. Y.; Cline, C. S.; Koker, E. B.; Carmichael, H. H.; Chignell, C. F.; Bilski, P. Quenching of Singlet Molecular Oxygen ($^1O_2$) by Azide Anion in Solvent Mixtures. *Photochem. Photobiol.* **2001**, *74*, 760−764.
(45) Sudlow, G.; Birkett, D. J.; Wade, D. N. The Characterization of Two Specific Drug Binding Sites on Human Serum Albumin. *Mol. Pharmacol.* **1975**, *11*, 824−832.
(46) Weller, A. Photoinduced Electron Transfer in Solution: Exciplex and Radical Ion Pair Formation Free Enthalpies and their Solvent Dependence. *Z. Phys. Chem. Neue Folge* **1982**, *133*, 93−98.
(47) Khan, T. A.; Hriljac, J. A. Hydrothermal Synthesis of Microporous Materials with the Direct Incorporation odf Porphyrin Molecules. *Inorg. Chim. Acta* **1999**, *294*, 179−182.
(48) Hambright, P.; Fleischer, E. B. The Acid-Base Equilibria, Kinetics of Copper Ion Incorporation, and Acid-Catalyzed Zinc Ion Displacement from the Water-Soluble Porphyrin $\alpha,\beta,\gamma,\delta$-Tetra(4-*N*-methylpyridyl)porphyrin. *Inorg. Chem.* **1970**, *9*, 1757−1761.
(49) Ishikawa, Y.; Yamashita, A.; Uno, T. Efficient Photocleavage of DNA by Cationic Porphyrin-Acridine Hybrids with the Effective Length of Diamino Alkyl Linkage. *Chem. Pharm. Bull.* **2001**, *49*, 287−293.
(50) Usui, Y.; Kamogawa, K. A Standard System to Determine the Quantum Yield of Singlet Oxygen Formation in Aqueous Solution. *Photochem. Photobiol.* **1974**, *19*, 245−247.

https://dx.doi.org/10.1021/acsomega.0c04303
ACS Omega 2020, 5, 27702−27708